Applied Surface Science 47 (1991) 195–203
North-Holland

Interdiffusion studies on high-T_c superconducting $YBa_2Cu_3O_{7-\delta}$ thin films on Si(111) with a $NiSi_2/ZrO_2$ buffer layer

W.A.M. Aarnink, D.H.A. Blank, D.J. Adelerhof, J. Flokstra, H. Rogalla, A. van Silfhout
University of Twente, P.O. Box 217, 7500 AE Enschede, Netherlands

and

R. de Reus
Risø National Laboratory, P.O. Box 49, DK-4000 Roskilde, Denmark

Received 7 October 1990; accepted for publication 17 December 1990

Interdiffusion studies on high-T_c superconducting $YBa_2Cu_3O_{7-\delta}$ thin films with thicknesses in the range of 2000–3000 Å, on a Si(111) substrate with a buffer layer have been performed. The buffer layer consists of a 400 Å thick epitaxial $NiSi_2$ layer, covered with 1200 Å of polycrystalline ZrO_2. $YBa_2Cu_3O_{7-\delta}$ films were prepared using laser ablation.

The $YBa_2Cu_3O_{7-\delta}$ films on the $Si/NiSi_2/ZrO_2$ substrates are of good quality; their critical temperatures $T_{c,zero}$ and $T_{c,onset}$ have typical values of 85 and 89 K, respectively. The critical current density j_c at 77 K equaled 4×10^4 A/cm^2. With X-ray diffraction analysis (XRD), only *c*-axis orientation has been observed.

The interdiffusion studies, using Rutherford backscattering spectrometry (RBS) and scanning Auger microscopy (SAM) show that the ZrO_2 buffer layer prevents severe Si diffusion to the $YBa_2Cu_3O_{7-\delta}$ layer, the Si concentration in the ZrO_2 layer must be below the detectability limit of 1 at%, but Si diffusion along grain boundaries cannot be excluded completely. During short deposition times ($t \approx 5$ min) no severe interface reactions occur. The interfaces are sharp and well defined. However, during long deposition times ($t > 30$ min), some Cu diffuses from the $YBa_2Cu_3O_{7-\delta}$ layer to the interface between the ZrO_2 layer and the $NiSi_2$ layer. Also indications for the formation of $BaZrO_3$ at the interface between the $YBa_2Cu_3O_{7-\delta}$ layer and the ZrO_2 layer have been found. Finally, Ni diffusion into the Si substrate and Ni segregation to the surface of the ZrO_2 layer may be expected.

From the results we may conclude that, when using laser ablation, it is well possible to grow polycrystalline, *c*-axis-oriented high-T_c superconducting $YBa_2Cu_3O_{7-\delta}$ thin films on a Si(111) substrate with a $NiSi_2/ZrO_2$ buffer layer.

1. Introduction

Since the discovery of high-T_c superconducting oxides [1], great efforts have been spent to fabricate thin films of these materials. Especially in the case of $YBa_2Cu_3O_{7-\delta}$, many groups succeeded in depositing high-quality thin films on various substrates, using different deposition techniques [2–7].

The possible integration of high-T_c superconducting and semiconducting devices on the same silicon substrate is of great interest. However, due to its high mobility, Si diffuses into the $YBa_2Cu_3O_{7-\delta}$ layer during deposition and deteriorates the superconducting properties considerably [8]. Also Ba can be expected to diffuse into the Si substrate [9]. To prevent these reactions between the Si substrate and the $YBa_2Cu_3O_{7-\delta}$ film, a buffer layer can be used. However, it must be possible to grow high-quality $YBa_2Cu_3O_{7-\delta}$ thin film on this buffer layer. Experiments show that on single-crystal yttrium-stabilized ZrO_2 (YSZ), $SrTiO_3$ and MgO substrates, effects of interface reactions can be minimized and high-quality $YBa_2Cu_3O_{7-\delta}$ thin films can be grown on these substrates [10,11]. In the literature it is also shown that YSZ thin layers can be grown epitaxially on

Si(100) substrates [12]. Therefore, it is of great interest to use a Si/ZrO_2 structure as a substrate for growing high-quality high-T_c superconducting $YBa_2Cu_3O_{7-\delta}$ thin films. Recently, results on $YBa_2Cu_3O_{7-\delta}$ thin films on Si with an epitaxial YSZ buffer layer have been reported [13].

Besides YSZ, also other materials may be used in buffer layers on Si [14]. In this paper we present results on interdiffusion studies of high-T_c superconducting $YBa_2Cu_3O_{7-\delta}$ thin films on a Si substrate with a buffer layer consisting of a $NiSi_2$ layer with a ZrO_2 layer on top. A combination of Rutherford backscattering spectrometry (RBS) and scanning Auger microscopy was used to analyse the multilayer structures. The $NiSi_2$ layer is grown epitaxially on the Si(111) substrate and has a thickness of about 400 Å in our experiments. The ZrO_2 layer with a thickness of about 1200 Å is polycrystalline. The $YBa_2Cu_3O_{7-\delta}$ layers with a typical thickness of 2000–3000 Å were deposited using laser ablation.

2. Experimental

In our interdiffusion studies we investigated diffusion and segregation effects in the preparation of $Si/NiSi_2/ZrO_2/YBa_2Cu_3O_{7-\delta}$ multilayer structures and studied the composition of interfaces in these structures in detail, combining different analysis techniques.

The $NiSi_2/ZrO_2$ buffer layer was prepared by oxidizing a 530 Å thick amorphous $Ni_{23}Zr_{77}$ layer, that was coevaporated onto a Si(111) single crystal in a dual electron gun evaporator. To form the buffer layer, the substrate with the $Ni_{23}Zr_{77}$ layer on top was annealed in a furnace for 2 h at 500 °C in 1×10^{-2} Pa O_2. During this treatment a 400 Å thick epitaxial $NiSi_2$ layer on the Si(111) substrate and a 1200 Å thick polycrystalline ZrO_2 top layer were formed simultaneously, see also ref. [15].

A set of $YBa_2Cu_3O_{7-\delta}$ layers was deposited on top of these buffer layers using laser ablation. The experimental set-up is described in ref. [10]. During deposition of the various layers only the laser pulse frequency was varied and, therefore, the deposition rate. Other parameters as the substrate temperature and O_2 pressure were not changed and adjusted to 720 °C and 30 Pa, respectively, during the preparation. In this way $YBa_2Cu_3O_{7-\delta}$ layers with similar thicknesses but different deposition times were prepared, allowing us to study time-dependent interdiffusion processes.

We performed experiments on four samples: (1) the virgin $Si/NiSi_2/ZrO_2$ substrate and (2) a $Si/NiSi_2/ZrO_2$ substrate, treated in the laser-ablation chamber. During the deposition of an $YBa_2Cu_3O_{7-\delta}$ layer, the substrate is heated. To simulate the effects of this heat treatment a virgin $Si/NiSi_2/ZrO_2$ substrate was annealed for 30 min at 720 °C in 30 Pa O_2. (3) The $Si/NiSi_2/ZrO_2$ substrate with an $YBa_2Cu_3O_{7-\delta}$ layer. For this layer the laser pulse frequency was set to 10 Hz. The deposition time was 6 min. (4) The $Si/NiSi_2/ZrO_2$ substrate, also with an $YBa_2Cu_3O_{7-\delta}$ layer on top of it, but in this case the laser pulse frequency was set to 2 Hz and the deposition time was 35 min.

X-ray diffraction analysis (XRD) was used to determine the structure and orientation of the $YBa_2Cu_3O_{7-\delta}$ layers and superconducting properties were derived from critical temperature T_c and critical current density j_c measurements.

For the interdiffusion studies, we used 2 MeV $^4He^+$ Rutherford backscattering spectrometry (RBS) and scanning Auger microscopy (SAM). RBS spectra were taken with a scattering angle and a sample tilt of 170° and 7°, respectively, and were analysed using the RUMP computer code [16]. The results of SAM were analysed using the ESAU program implemented on a PDP 11 computer controlling the PHI Multiprobe 600 system [17]. The base pressure of this system is 3×10^{-8} Pa. The Auger spectra, depth profiles and line profiles were taken using a 10 keV electron beam with a typical beam current of 0.5 μA. For the ion etching 3.5 keV Ar^+ ions were used. During calibration the Ar^+ ion gun is aligned with the electron beam, so that depth profiles are taken at the center of the sputter crater (see fig. 1). The sputter rate has been calibrated using a Ta_2O_5 layer with a thickness of 1000 Å, grown on a Ta substrate. Also the results of RBS measurements have been used to determine the sputter rate of the Ar^+ ion gun. With the instrumental settings, used for taking the Auger sputter profiles, the

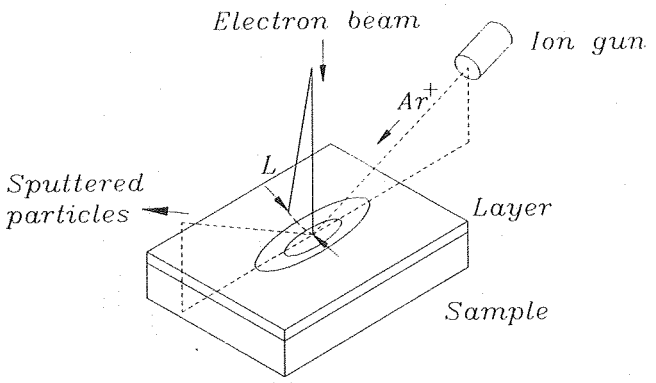

Fig. 1. Crater-edge Auger line profiling. Interfaces are stretched and, therefore, can be studied in detail.

detectability limits for Si, Ni and Cu equaled 1.0 at% Si, 0.5 at% Ni and 0.5 at% Cu, respectively [18]. For crater-edge profiling, line profiles were recorded at the sputter crater edge along curve L (fig. 1). Calculations show (see section 4) that the angle between the normal to the sample surface and the normal to the surface of the crater edge equals $\simeq 0.06°$. Therefore, interfaces are stretched at the crater edge and can be studied in detail.

3. Results

The $YBa_2Cu_3O_{7-\delta}$ layers deposited on the Si substrates with a $NiSi_2/ZrO_2$ buffer layer are of good quality. In the XRD analysis only the (00*l*) reflections can be seen, showing that the films are perfectly *c*-axis-oriented. In the measured $\rho-T$ curve of sample 4 (see fig. 2) the critical temperatures $T_{c,zero}$ and $T_{c,onset}$ reach values of 85 and 89

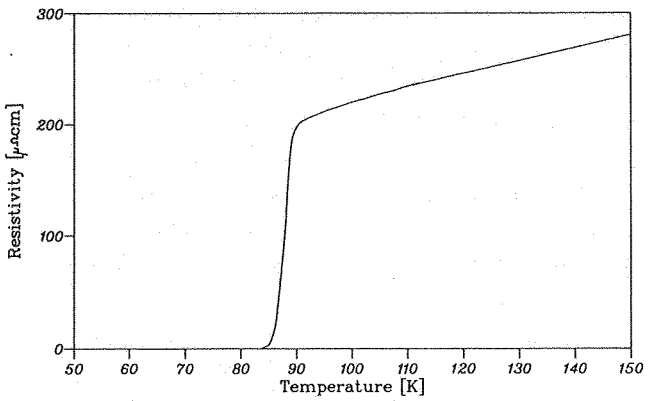

Fig. 2. $\rho-T$ curve of $YBa_2Cu_3O_{7-\delta}$ layer (sample 4), deposited on a Si substrate with a $NiSi_2/ZrO_2$ buffer layer using laser ablation.

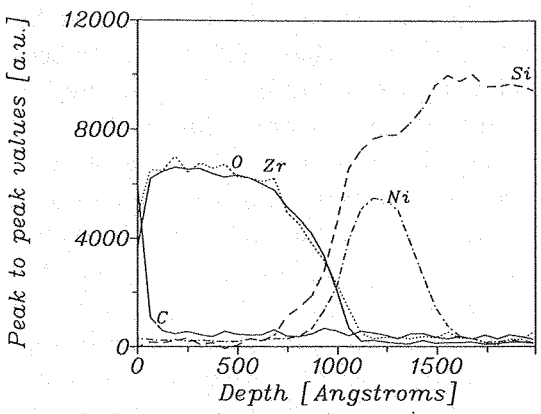

Fig. 3. Auger sputter profile of the virgin buffer layer, sample 1.

K, respectively. The critical current density j_c at 77 K is 4×10^4 A/cm^2 measured with criterion of a 1 μV on a bridge of 10 μm width and 100 μm length. It has to be noted that these results are typical results: for an elaborate parameter study we refer to ref. [10].

3.1. Interdiffusion studies using SAM and RBS

In fig. 3 the Auger sputter profile of sample 1, the virgin $Si/NiSi_2/ZrO_2$ substrate, is given. This measurement shows sharp, well-separated elemental profiles, which are indicative of sharp and well-defined interfaces. No diffusion of Si into the ZrO_2 layer could be observed. An Auger spectrum, taken on the surface, revealed a small Ni concentration of 1 at% in the top layer (thickness < 50 Å). Below this top layer, no Ni could be detected in the ZrO_2 layer. With RBS measurements the thickness of the $NiSi_2$ and ZrO_2 layers were found to be about 400 and 1200 Å, respectively. By means of RBS channeling experiments it was found that the $NiSi_2$ layer is epitaxial with the Si(111) substrate [15]. The ratio of the atomic concentrations of Ni and Si equaled 0.50. The C contamination at the surface of the buffer layer (fig. 3) is expected to be due to transport from the deposition chamber through the ambient to the PHI Multiprobe 600 system.

The RBS spectrum of the treated $Si/NiSi_2/ZrO_2$ substrate (sample 2) is given in fig. 4. Analysing it we found that the $NiSi_2$ layer had a thickness of about 400 Å and that it was slightly

enriched with Si. The atomic ratio of Ni and Si was found to be 0.40. These differences, when compared with the virgin buffer layer, are due to Ni diffusion into the Si substrate during the heat treatment. The thickness of the ZrO_2 layer, was determined as 1100 Å. With Auger sputter profiling no Si diffusion into the ZrO_2 could be detected. On top of the ZrO_2 layer some Ni can be observed: a small increase in the backscattered yield at the Ni surface channel can be seen in fig. 4. An Auger survey scan showed a 3 at% Ni concentration in the surface layer of the ZrO_2 layer. With Auger sputter profiling no Ni was observable in the ZrO_2 below this surface layer (thickness < 50 Å).

The RBS spectrum of sample 3 is given in fig. 5. The broadening of the Ni peak at the low energy side near channel 220 is indicative of a little bit of Ni diffusing into the Si substrate during deposition of the $YBa_2Cu_3O_{7-\delta}$ layer, which is confirmed by the decrease in the rising edge of Si near channel 150. Since the yield drops nearly to zero above channel 160 we conclude that no severe Si diffusion into the ZrO_2 layer has occurred. With Auger sputter profiling this result was confirmed. In the ZrO_2 layer no Si was observed. The backscattered yield near channel 240, between the Ni and Zr peak, has increased when compared with the virgin and the treated buffer layer. The interface between the $NiSi_2$ and the ZrO_2 layer may be degraded somewhat due to

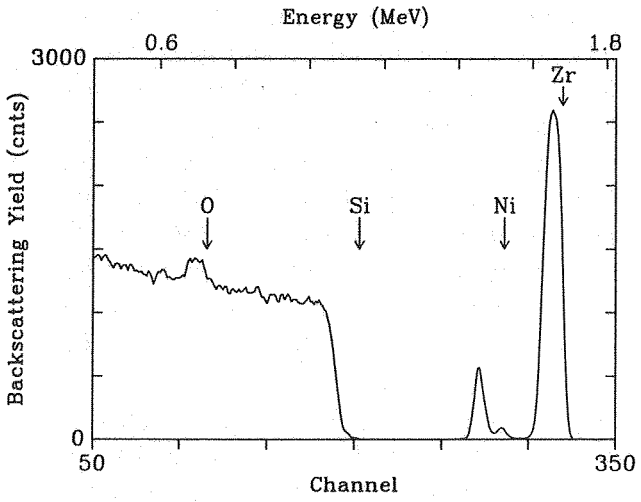

Fig. 4. RBS spectrum of the annealed buffer layer, sample 2.

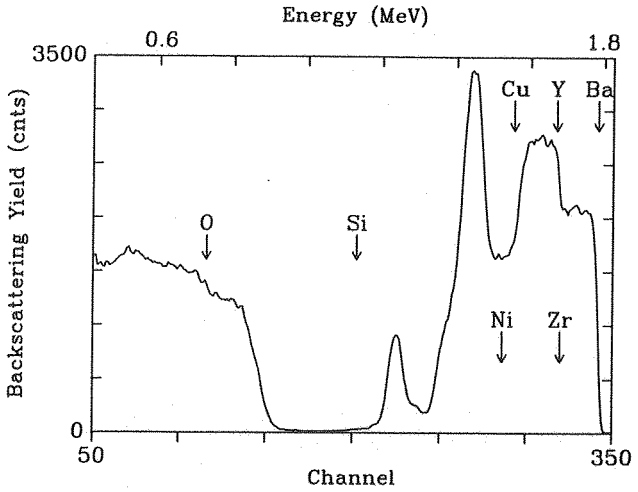

Fig. 5. RBS spectrum of sample 3. The laser-pulse frequency was set to 10 Hz and the deposition time of the $YBa_2Cu_3O_{7-\delta}$ layer was 6 min.

intermixing of Ni and Zr at this interface during deposition of the $YBa_2Cu_3O_{7-\delta}$ layer. From the trailing edge of the Ba peak near channel 300 and the rising edge of Zr peak near channel 270, we may exclude that severe interface reactions have taken place at the interface between the ZrO_2 and $YBa_2Cu_3O_{7-\delta}$ layer: no severe interdiffusion of Ba and Zr has occurred. The thickness of the $NiSi_2$ layer equaled 400 Å, the thickness of the ZrO_2 layer 1100 Å and the thickness of the $YBa_2Cu_3O_{7-\delta}$ layer was found to be 1900 Å. As in the case of sample 2 the $NiSi_2$ layer is slightly enriched with Si, the atomic ratio of Ni to Si equalling 0.40.

The Auger sputter profile and RBS spectrum of sample 4 are shown in figs 6 and 7, respectively. Before taking the Auger sputter profile a 1000 Å thick layer was sputtered away. The thickness of the $NiSi_2$ layer equals 400 Å. The Si profile, especially the little shoulder near the $NiSi_2/ZrO_2$ interface may indicate a Si enrichment of the $NiSi_2$ layer. From the Zr, Si and Ni profile we can see that at the $NiSi_2/ZrO_2$ interface some reaction has taken place. The Zr, Si and Ni have interdiffused there. Also close examination of the Cu region data, taken during profiling, revealed that at the $NiSi_2/ZrO_2$ interface about 5 at% Cu is present. As will be shown in section 3.2 this is due to Cu diffusing from the $YBa_2Cu_3O_{7-\delta}$ layer through the ZrO_2 layer. At the ZrO_2/YBa_2Cu_3

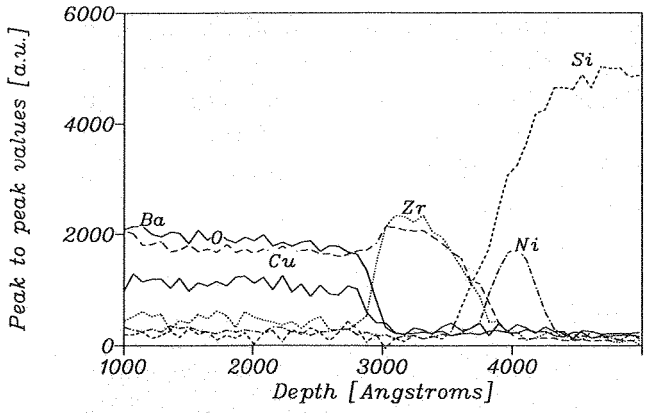

Fig. 6. Sputter profile of sample 4. Before taking this profile, 1000 Å of the $YBa_2Cu_3O_{7-\delta}$ layer was sputtered away. The laser-pulse frequency was set to 2 Hz and the deposition time of the $YBa_2Cu_3O_{7-\delta}$ layer was 35 min.

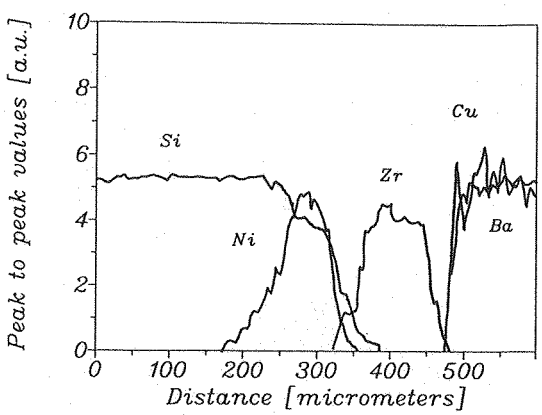

Fig. 8. Line profiles on crater edge in sample 3. See also fig. 1. The laser-pulse frequency was set to 10 Hz and the deposition time of the $YBa_2Cu_3O_{7-\delta}$ layer was 6 min.

$O_{7-\delta}$ interface no strong interface reactions can be observed in the sputter profile (fig. 6).

In the RBS spectrum (fig. 7) of sample 4 we observe an interface reaction at the $NiSi_2/ZrO_2$ interface, the backscattered yield near channel 220 between the Ni and Zr peak, has increased. As will be shown by the results of crater-edge Auger line profiling, this can be attributed partly to Cu diffusing from the $YBa_2Cu_3O_{7-\delta}$ layer through the ZrO_2 layer towards the $NiSi_2/ZrO_2$ interface. Besides this Cu diffusion, the interface has degraded due to interdiffusion of Zr and Ni. Finally, we conclude that some interface reaction has taken

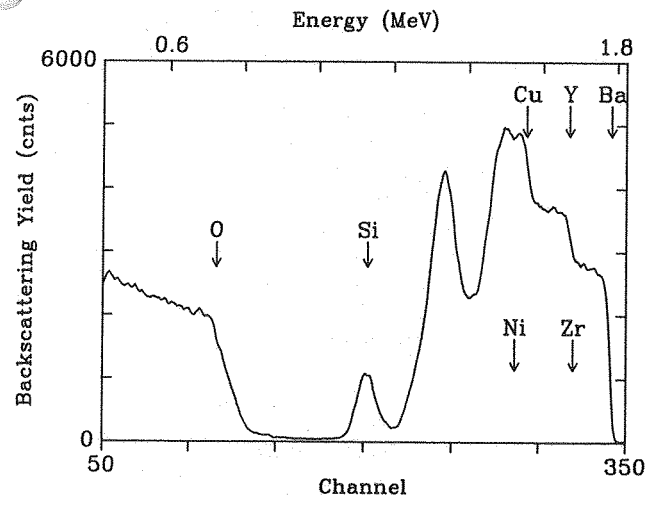

Fig. 7. RBS spectrum of sample 4. The laser-pulse frequency was set to 2 Hz and the deposition time of the $YBa_2Cu_3O_{7-\delta}$ layer was 35 min.

place at the $ZrO_2/YBa_2Cu_3O_{7-\delta}$ interface. This is noticed best by a decrease in yield and a broadening of the Zr peak, which is found near channel 250. Also the trailing edge of the Ba peak near channel 280 is broadened. Most likely some $BaZrO_3$ is formed. The $NiSi_2$ layer with a thickness of 400 Å was slightly enriched with Si. The atomic ratio of Ni to Si was again found to be 0.40. The thicknesses of the ZrO_2 layer and the $YBa_2Cu_3O_{7-\delta}$ layer were determined as 1100 and 2800 Å, respectively.

3.2. *Interface properties, studied by crater-edge profiling*

To obtain detailed information about the reactions that have taken place at the interfaces, we performed crater-edge Auger line profiling (see fig. 1) and the results for sample 3 and 4 are given in figs. 8 and 9.

In fig. 8 the crater-edge Auger line profiles of sample 3 are given. According to the Ni profile, a little Ni diffusion into the Si substrate took place. From the Si profile, we see that no Si diffused into the ZrO_2 layer. For Cu and Ba the line profiles show that the $ZrO_2/YBa_2Cu_3O_{7-\delta}$ interface is sharp and well defined. No interface reactions have taken place during the deposition of the $YBa_2Cu_3O_{7-\delta}$ layer.

The Auger line profiles of sample 4 at the crater edge are given in fig. 9. From the Ni line profile some diffusion of Ni into the Si substrate

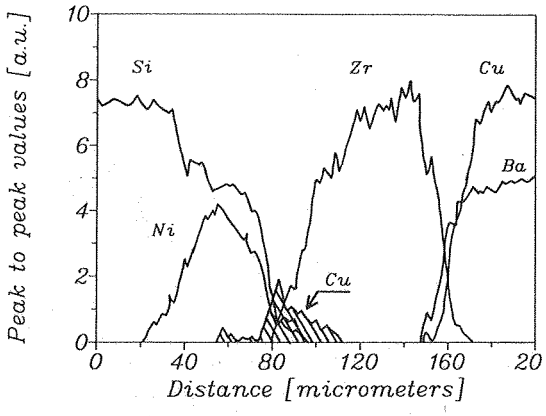

Fig. 9. Line profiles on crater edge in sample 4. See also fig. 1. The laser-pulse frequency was set to 2 Hz and the deposition time of the $YBa_2Cu_3O_{7-\delta}$ layer was 35 min. Note the Cu at the $NiSi_2/ZrO_2$ interface.

may be expected. From the Si profile we see no diffusion of Si into the ZrO_2 layer. From the Ba line profile we see a well-defined interface, however, some mixing with Zr can be observed, indicating the formation of $BaZrO_3$. The Cu line profile reveals a Cu deficiency in the $YBa_2Cu_3O_{7-\delta}$ layer near the $ZrO_2/YBa_2Cu_3O_{7-\delta}$ interface. From the line profiles the thickness of this Cu-deficient layer can be estimated to be 300 Å. The Cu that is missing here diffused through the ZrO_2 layer towards the $NiSi_2/ZrO_2$ interface, as can be seen in the Cu line profile very clearly. For the $NiSi_2$ layer being enriched with Si, probably some copper silicide [19] has been formed at the $NiSi_2/ZrO_2$ interface during deposition of the $YBa_2Cu_3O_{7-\delta}$ layer.

4. Discussion

XRD, measurements of the critical temperature T_c and the critical current density j_c showed that the $YBa_2Cu_3O_{7-\delta}$ layers deposited on silicon substrates with a buffer layer are of good quality [10]. Comparable results have been obtained by other authors [20,21], but they used a Si/ZrO_2 or a $Si/SiO_2/ZrO_2$ structure as a substrate, whereas here $Si/NiSi_2/ZrO_2/YBa_2Cu_3O_{7-\delta}$ multilayer structures are prepared. In this structure, the ZrO_2 layer is polycrystalline. With epitaxial YSZ buffer layers on Si, results improve [13]. Our multilayer structure has the advantage that the $NiSi_2$ may be used for electrical contacts or as a counter electrode. As can be seen from the results in section 3 the $NiSi_2$ is not well suited as a buffer layer for Si, although it may influence the microstructural

Table 1
Summarized results of interdiffusion studies

Sample	Description	Layer thicknesses			Observations using RBS, SAM and crater-edge profiling
		$NiSi_2$ (Å)	ZrO_2 (Å)	$YBa_2Cu_3O_{7-\delta}$ (Å)	
1	Virgin $Si(111)/NiSi_2/ZrO_2$ structure	400	1200	–	Little Ni at surface layer of ZrO_2 (< 1 at%)
2	$Si(111)/NiSi_2/ZrO_2$ structure, annealed for 30 min in 30 Pa O_2 at 720 °C	400	1140	–	Ni in surface layer of ZrO_2 (≃ 3 at%) Little Si enrichment of $NiSi_2$ layer: at%Ni/at%Si = 0.40 Ni diffusion into Si substrate
3	$Si(111)/NiSi_2/ZrO_2/YBa_2Cu_3O_{7-\delta}$ structure, deposition of $YBa_2Cu_3O_{7-\delta}$ layer took 6 min	400	1100	1900	Si enrichment of $NiSi_2$ layer: at%Ni/at%Si = 0.37 Ni diffusion into Si substrate
4	$Si(111)/NiSi_2/ZrO_2/YBa_2Cu_3O_{7-\delta}$ structure, deposition of $YBa_2Cu_3O_{7-\delta}$ layer took 35 min	400	1070	2850	Si enrichment of $NiSi_2$ layer: at%Ni/at%Si = 0.37 Ni diffusion into Si substrate Cu diffusion from $ZrO_2/YBa_2Cu_3O_{7-\delta}$ to $NiSi_2/ZrO_2$ interface Formation of $BaZrO_3$ at $ZrO_2/YBa_2Cu_3O_{7-\delta}$ interface

properties of the polycrystalline ZrO_2 buffer layer and, therefore, increase its density. The results of the interdiffusion studies are summarized in table 1.

The way buffer layers were prepared yields a $Si/NiSi_2/ZrO_2$ multilayer structure in which the $NiSi_2$ and the ZrO_2 are well separated and in which the interfaces are well defined. The ZrO_2 layer prevents severe Si diffusion into the layer on top of it; after preparation no Si could be observed in the polycrystalline ZrO_2 layer with SAM (detectability limit: 1 at% Si [18]).

In the annealed buffer layer some Ni diffused into the Si substrate. Also the Ni atomic concentration at the surface of the ZrO_2 layer increased. In the ZrO_2 layer no Ni was detected (detectability limit: 0.5 at% Ni [18]). From the results we conclude that Ni segregated towards the surface of the ZrO_2 layer during the anneal. As for the virgin buffer layer also after the anneal no Si in the ZrO_2 layer could be detected using Auger sputter profiling. In another study [10] we showed by Auger line profiling that in a buffer layer that consists only of polycrystalline ZrO_2, some Si diffuses only along the grain boundaries in the ZrO_2 layer. No Si could be detected in the $YBa_2Cu_3O_{7-\delta}$ thin film on top of this buffer layer. This ZrO_2 buffer layer was deposited using RF-magnetron sputtering, followed by an anneal in O_2 ambient at 500 °C. The $NiSi_2/ZrO_2$ buffer layer presented here was prepared differently, see section 2. This may have influenced the density of the ZrO_2 layer and the number of grain boundaries in this layer, leading to a more dense ZrO_2 layer in the $Si/NiSi_2/ZrO_2$ structure.

For short deposition times ($t \approx 5$ min) of the $YBa_2Cu_3O_{7-\delta}$ top layer no interface reactions could be observed. However, for long deposition times ($t > 30$ min) we found that the Ni to Si atomic ratios decrease. These decreased atomic ratios are averaged over the detection volume. It may be due to some Ni diffusion into the Si substrate. Also it is well possible that $NiSi_2$ islands are embedded in Si-rich regions. We found indications that some $BaZrO_3$ forms at the $ZrO_2/YBa_2Cu_3O_{7-\delta}$ interface, whereas some Cu diffused from the $YBa_2Cu_3O_{7-\delta}$ layer to the $NiSi_2/ZrO_2$ interface, indicating the formation of some copper silicide [19]. In the ZrO_2 layer no Cu could be detected (detectability limit: 0.5 at% Cu [18]). The observation of Cu diffusing through the ZrO_2 buffer layer has not been reported before and must be paid special attention when employing a deposition technique for $YBa_2Cu_3O_{7-\delta}$ thin films using a small deposition rate. In order to grow good-quality high-T_c superconducting $YBa_2Cu_3O_{7-\delta}$ thin films on the $NiSi_2/ZrO_2$ buffer layer, the deposition rate should be larger than 10 Å/min, otherwise a non-superconducting Cu-deficient film will be formed containing some $BaZrO_3$.

The diffusion of Cu and segregation of Ni which are reported here are expected to take place along the grain boundaries in the polycrystalline ZrO_2 layer. The elemental compositions of the interfaces as detected with Auger survey scans and sputter profiling strongly depend on the composition of the grain boundaries in the layer. In the ZrO_2 layer itself the intensities of Auger electrons emitted from the elements present in the grain boundaries, are below the detectability limit of about 0.5 at% [18] averaged over the whole detection volume when, as in our case, the typical diameter of the grains is large when compared to the width of the grain boundaries. In our case the diameter of the grains is typically 1 μm and, since reasonable critical current densities have been achieved, the thickness of the grain boundaries is not to be expected over a few nm. This explains the fact that in the ZrO_2 layer we did not detect Cu or Ni, although they diffused or segregated through the layer along the grain boundaries and still may be present there. In this way, also Si can diffuse along the grain boundaries into the ZrO_2 layer without detecting it with Auger sputter profiling. The results of our interdiffusion studies exclude severe Si diffusion into the $YBa_2Cu_3O_{7-\delta}$ layer, but Si diffusion along grain boundaries cannot be excluded completely. In this way, the critical current density j_c of the $YBa_2Cu_3O_{7-\delta}$ thin films is strongly dependent on the microstructural properties of the polycrystalline ZrO_2 buffer layer. Decreasing the number of grain boundaries in the ZrO_2 buffer layer will greatly improve the critical current density j_c of the $YBa_2Cu_3O_{7-\delta}$ thin film on top of it.

With Auger crater-edge profiling we are able to

stretch the interfaces by about a factor of 1×10^3. Knowing the thickness of the ZrO_2 layer the tangent of the angle between the normal to the sample surface and the normal to the crater-edge surface (see fig. 1) can be calculated from figs. 8 and 9 and equals $\simeq 0.001$. In this way very detailed information about the composition of interfaces can be obtained, although also with this technique the detectability limit of elements is typically 1 at% [18].

In the $Si/NiSi_2/ZrO_2/YBa_2Cu_3O_{7-\delta}$ multilayer structure the $NiSi_2$ may be used for electrical contacts or as a counter electrode. Also the use of a $NiSi_2$ layer may influence the microstructural properties of the polycrystalline ZrO_2 layer, leading to the formation of a buffer layer with higher density when compared to a polycrystalline ZrO_2 layer deposited on a Si substrate directly, and therefore reducing Si diffusion to the $YBa_2Cu_3O_{7-\delta}$ film. The results discussed here have been obtained on a polycrystalline ZrO_2 buffer layer. With epitaxial ZrO_2 buffer layers results improve [13].

5. Conclusions

A layer of $NiSi_2$ with a thickness of 400 Å, epitaxial to a Si(111) substrate, with a polycrystalline ZrO_2 top layer with a thickness of 1200 Å is well suited as a substrate for high-T_c superconducting $YBa_2Cu_3O_{7-\delta}$ thin films, using laser ablation as a deposition technique.

The combination of Rutherford backscattering spectroscopy and scanning Auger microscopy turned out to be a very valuable tool for studying interdiffusion processes in multilayer structures, yielding detailed insight in effects of reactions, diffusion and segregation on the structure and composition of the different interfaces.

Applying these techniques we saw that the ZrO_2 layer stops severe Si diffusion into the $YBa_2Cu_3O_{7-\delta}$ layer. Even with a detectability limit of 1 at% Si, no Si can be detected in the ZrO_2 layer or the $YBa_2Cu_3O_{7-\delta}$ layer. However, Si diffusion along the grain boundaries cannot be excluded completely. For short deposition times ($t \approx 5$ min) of the $YBa_2Cu_3O_{7-\delta}$ layer, the interfaces in the $Si/NiSi_2/ZrO_2/YBa_2Cu_3O_{7-\delta}$ multilayer structure are sharp and well defined, and no severe interdiffusion or interface reactions were observed.

However, with long deposition times ($t > 30$ min), some Cu diffuses from the bottom of the $YBa_2Cu_3O_{7-\delta}$ layer to the interface between the ZrO_2 and the $NiSi_2$ layer. Also indications for the formation of some $BaZrO_3$ at the interface between the $YBa_2Cu_3O_{7-\delta}$ and the ZrO_2 layers have been found. Finally, Ni diffusion into the Si substrate and Ni segregation through the ZrO_2 layer to the $ZrO/YBa_2Cu_3O_{7-\delta}$ interface must be expected.

Acknowledgements

This work is part of the research program of the "Stichting voor Fundamenteel Onderzoek der Materie (FOM)", which is financially supported by the "Nederlandse organisatie voor Wetenschappelijk Onderzoek (NWO)", and was made possible by support of the "FOM-Instituut voor Atoom and Molecuul Fysica (AMOLF)", Amsterdam, and the "Centrum voor Materialen Onderzoek (CMO)", Enschede.

References

[1] J.G. Bednorz and K.A. Müller, Z. Phys. B 64 (1986) 189.
[2] R.B. Laibowitz, R.H. Koch, P. Chaudhari and R.J. Gambino, Phys. Rev. B 35 (1987) 8821.
[3] M. Niato, R.H. Hammond, B. Oh, M.R. Beasley and T.H. Geballe, Appl. Phys. Lett. 51 (1987) 713.
[4] D. Dijkkamp, T. Venkatesan, X.D. Wu, S.A. Shaheen, N. Jisrawi, Y.H. Minlee, W.L. McLean and M. Croft, Appl. Phys. Lett. 51 (1987) 619.
[5] X.X. Xi, G. Linker, O. Meyer, E. Nold, B. Obst, F. Ratsel, R. Smithey, B. Strahlan, F. Weschenfilder and J. Geerd, Z. Phys. B (Condens. Matter) 74 (1989) 13.
[6] N. Missert, R. Hammond, J.E. Mooij, V. Matijasevic, P. Rosenthal, T.H. Geballe, A. Kapitulnik, M.R. Beasley, S.S. Laderman, C. Lu, E. Garwin and R. Barton, IEEE Trans. Magn. MAG-25 (1989) 2418.
[7] B. Roas, L. Schultz and G. Endres, Appl. Phys. Lett. 53 (1988) 1557.
[8] A. Mogro-Campero, B.D. Hunt, L.G. Turner, M.C. Burell and W.E. Balz, Appl. Phys. Lett. 52 (1988) 584.
[9] P. Madakson, J.J. Cuomo, D.S. Yee, R.A. Roy and G. Scilla, J. Appl. Phys. 63 (1988) 2046.

[10] D.H.A. Blank, D.J. Adelerhof, J. Flokstra and H. Rogalla, Physica C 167 (1990) 423.
[11] J. Gao, B. Häuser and H. Rogalla, J. Appl. Phys. 67 (1990) 2512.
[12] H. Fukumoto, T. Imura and Y. Osaka, Jpn. J. Appl. Phys. 27 (1988) L1404.
[13] D.K. Fork, D.B. Fenner, R.W. Barton, J.M. Phillips, G.A.N. Connel, J.B. Boyce and T.H. Geballe, Appl. Phys. Lett. 57 (1990) 1161.
[14] R. de Reus, F.W. Saris, G.J. van der Kolk, C. Witmer, B. Dam, D.H.A. Blank, D.J. Adelerhof and J. Flokstra, Mater. Sci. Eng. B 7 (1990) 135.
[15] R. de Reus, H.C. Tissink and F.W. Saris, J. Mater. Res. 5 (1990) 341.
[16] L.R. Doolittle, Nucl. Instr. Meth. B 9 (1985) 344.
[17] PHI Multiprobe 600/595 Videotape Guide, Physical Electronics Division, Perkin-Elmer.
[18] Detectability Limits for Auger Analysis, PHI Technical Bulletin No. T8401 (5/5/84), Physical Electronics Division, Perkin-Elmer.
[19] C.-A. Chang, J. Appl. Phys. 67 (1990) 566.
[20] A. Mogro-Campero, L.G. Turner and G. Kendall, Appl. Phys. Lett. 53 (1988) 2566.
[21] T. Venkasesan, E.W. Chase, X.D. Wu, A. Inam, C.C. Chang and F.K. Shokoohi, Appl. Phys. Lett. 53 (1988) 243.